Design-Informatics Approach Applicable to Real-World Problem

Kazuhisa Chiba
Department of Mechanical Systems Engineering
Hokkaido Institute of Technology
Sapporo 006–8585, Japan
Email: thousandleaf@gmail.com

Yoshikazu Makino and Takeshi Takatoya
Aviation Program Group
Japan Aerospace Exploration Agency
Tokyo 182–8522, Japan

***Abstract*—The *design-informatics approach* has been proposed for next-generation innovative design methodology. The multi-objective problem should be treated in a real-world engineering problem because of the various design requirements. When a multi-objective optimization is implemented, the obtained result is not a sole solution but a set of optimum solutions due to tradeoff relations among design requirements. Therefore, decision-making process is necessary as a post-process for optimization result. In the present study, the design-informatics approach, which is considered as a sequential process between an optimization and its post-process operations, is suggested and is applied to the large-scale and real-world design problem. Consequently, a compromised solution can be efficiently decided from the non-dominated solutions obtained by multidisciplinary design optimization. This approach would be a new efficient procedure for design manner, and also it would be the methodology that innovative design knowledge can be acquired.**

I. Introduction

Design-informatics approach composed by optimization and data mining as a decision-making process is the efficient design methodology. Especially, it is effective to the design of aerospace vehicle which is a large-scale and real-world problem and has the evaluations with troubles for many design requirements. The word as large scale mentioned here has two senses as follows; a) the huge time to evaluate objective functions on high-fidelity is needed, b) the many design variables are necessary for the definition of intimate configuration. When the large-scale problem as a) is considered, approximation methods typified as a response surface method can resolve it[1]. However, when the large-scale problem as b) is considered, it is difficult to manage the problem. When Design of Experiments approach (DoE) is employed, many sample points should be generally evaluated to cover design-variable space due to many design variables. That is, there is no congeniality between DoE and the problem with many design variables. It is also difficult that response surface model based on DoE apply to that problem. Therefore, heuristic algorithms typified as evolutionary algorithms should be selected for the optimization problems with a large number of design variables. One of the reasons is that heuristic algorithms can efficiently explore vast design space with independence of objective functions. Another reason is that each design objective should be managed as independent objective functions to obtain tradeoff information (Pareto solutions) in multi-objective (MO) optimization problem. Therefore, heuristic algorithms should be employed for a large-scale optimization problem. But, sufficiently evolved solutions are not achieved due to the time restraint. In the case of the present study, it took roughly seven days at least for one generation. As the order of the fourth power of 10 at least is necessary for sufficient evolution in the information science field, it should visionary take 20 years for the present optimization. Consequently, even when an optimization is performed by using maximum period as much as possible, it is difficult to acquire the solution with which designers are satisfied from its result. Thus, the operation as data mining is carried out for the set of solutions obtained by an optimization. Since, this operation stipulates the design information existed in design space, a desirable final compromise solution would be conducted from an optimization result. The design information is as follows; 1) tradeoffs among objective functions, 2) correlations among objective functions, design variables, and characteristic performances, 3) experience and scent considered unconsciously during the definition of an optimization problem, 4) the flaw in the definition of an optimization problem. In addition, as the design information would have the knowledge that designers never consider, it would yield the seed for an innovative design. This study denominates a sequence of the present methods on optimization and data mining the design informatics approach. And then, the systematic management would be proposed. In addition, this approach is applied for the silent supersonic technology demonstrator[2] so that a compromise solution is determined.

II. Design-Informatics Approach

Figure 1 shows the flowchart of the present design-informatics approach. The design problem is firstly defined such as objective functions, constraints, and design space. And then, optimization is implemented to obtain non-dominated solutions for database construction. When non-dominated solutions are lopsidedly in design space, response surface method is frequently used to uniform the location of solutions. In this study, the obtained non-dominated solutions were directly employed as the design database not to use approximations. For generated design database, data mining is performed to extract useful design knowledge. Of course, not only non-

Definition of design problem

↓

Acquisition of non-dominated solutions using optimization

↓

Construction of database using derived non-dominated solutions

↓

Extraction of design knowledge using data mining

Fig. 1. Flowchart of the design-informatics approach.

dominated solutions but also all solutions can be employed as database, but non-dominated solutions are used in this study to efficiently select a beneficial compromise solution. It is confirmed that the design knowledge obtained from non-dominated solutions is connoted that acquired from all solutions[3].

A. Multidisciplinary Design Optimization

Since a real-world engineering problem has design objectives (objective functions) around multiple field, an MO design optimization (MDO) should be implemented. An MDO can have been performed for a large-scale problem (for example it roughly takes over 20 hours for aerodynamic evaluation in one case!) due to the recent progress of computer. MDO, which carries out not conceptual-design like optimization definition but a detailed and practical problem definition, is needed to apply a consequent compromise solution which design-informatics approach gives for practical product. The present MDO is performed among aerodynamics, stability, structures, aeroelasticity, and boom noise.

1) Optimizer: A hybrid method[4], [5] between MO particle swarm optimization (PSO) and the adaptive range MO genetic algorithm (GA) is employed. As the hybritization is only the archive sharing, PSO and GA are completely independent. It was confirmed to have better characteristics for a large-scale optimization[4].

Although a response surface model as, for example, the Kriging statistical surrogate model[6], [7] can be employed, it is not selected in the present application because surrogate model cannot deal with a large number of design variable. In addition, since the designers require to present many exact optimum solutions for the decision of a compromise one, an evolutionary-based Pareto approach as an efficient multi-thread algorithm is employed instead of gradient-based method.

B. Data Mining

Although a design optimization is important for engineering, the most significant point is the extraction of the knowledge in design space. The results obtained by MO optimization are not a sole solution but an optimum set. That is, as MO optimization result is insufficient information for practical design because designers need a conclusive shape. However, the result of MO optimization can be accounted as a hypothetical design database. Data mining as a post-process for an optimization is essential to obtain the fruitful design knowledge efficiently[8], [9]. That is, MO optimization and data mining should be unify to handle as an efficient design manner. A sequence of systemized system would be called as design-informatics approach. In the present study, functional analysis of variance[10], [11] (ANOVA) and self-organizing map[12] (SOM) are used as data mining technique. The distinguishing feature of a self-organizing map is the generation of a qualitative description. The advantage of this method includes the intuitive visualization of two-dimensional colored maps of design space using bird-eye-like views. As a result, SOM directly reveals the tradeoffs among objective functions. Moreover, SOMs roughly address the effective design variables and also reveal how a specific design variable affects objective functions and other design characteristics. However, SOM is subjective due to color cognizance. There is also a possibility of oversight because of a large number of objective functions and design variables. On the other hand, the distinguishing property of ANOVA is the quantitative description. The advantage of this method is the fact that it directly finds globally effective design variables. But, ANOVA cannot directly identify the effects of design variables on objective functions. When two methods are combined together, the results obtained can compensate with the disadvantages of the individual methods[3]. In the present study, mining by SOM is performed after key design variables are addressed by ANOVA.

III. Application and Its Result

Since the flight experiment of the non-powered supersonic experimental scaled airplane NEXST-1 was succeeded in October 2005[13], the supersonic technology demonstrator (S^3TD) then has been researching and developing as a next step in Japan Aerospace Exploration Agency (JAXA). In the previous work, the 2nd shape was redesigned[14]. The purpose of the previous work was the decision of the main wing planform using the multidisciplinary design exploration. The design requirements included the lift, friction drag. The structural requirements were defined by the strength and vibration of the main wing. In addition, the design configuration was simply

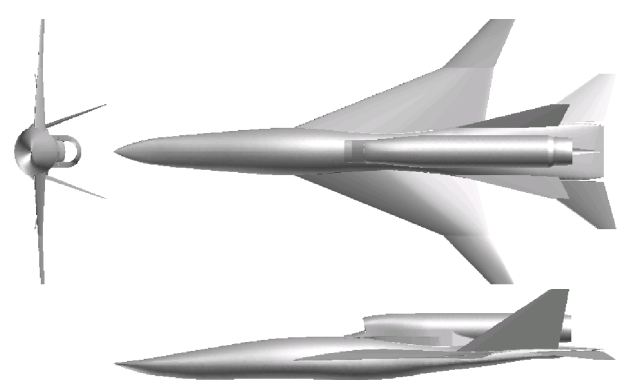

Fig. 2. Three views for the intimate configuration of 2.5th shape.

wing-fuselage configuration. On the other hand, the purpose of the present study is the design of the three-dimensional main wing and the security of the body stability and the 3rd shape is updated. The design requirements do not investigate the lift and the friction drag due to the fixed planform shape but add the stability. The structural requirements are defined by the strength and flutter of the main wing. Moreover, the design configuration is strictly an intimate configuration constructed as the main wing, fuselage, vertical tail wing, stabilizer, and engine system to evaluate the trim performance and accurate rear boom intensity as shown in Fig. 2.

The objective of the application is to design the 3rd intimate configuration of the S^{3}TD using the design-informatics approach, using computational fluid dynamics and computational structural dynamics evaluation tools, on the hybrid optimizer. Moreover, the design information for the S^{3}TD is extracted from the optimization result by using data mining, the decision making is then implemented, *i.e.*, a compromise solution is determined through the designers' discussion using extracted design knowledge.

A. Problem Definition

1) Objective Functions:

1) The minimization of the pressure drag coefficient C_{D_p} at the supersonic cruising condition, which is defined as Mach number of 1.6, altitude of 14km, and target lift coefficient C_L of 0.055. The target C_L is constant due to the fixed planform.
2) The minimization of the intensity of sonic boom I_{boom} at the supersonic cruising condition. This objective function value is defined as $|\Delta P_{\max}| + |\Delta P_{\min}|$ at the location with largest (smallest if negative) peak of sonic-boom signature across boom carpet. Note that $\Delta P_{\max}$ and $\Delta P_{\min}$ are front- and rear-boom intensity, respectively.
3) The minimization of the structural weight W for a main wing. The inboard and outboard wings are respectively defined as metal and composite materials. The minimum wing weight is solved with the fulfillment of the strength and flutter requirements. For the inboard wing made of metal, the thicknesses of skin and multi-frames are optimized. In addition, for the outboard wing made of composite material, the stacking sequence is optimized. These are the combination optimizations, and these are the nesting constitution for the present MDO.
4) The minimization of the difference between the centers of pressure and of gravity $|x_{\text{cp}} - x_{\text{cg}}|$ to trim, *i.e.*, trim performance. Note that MAC denotes mean aerodynamic chord. The center of pressure is calculated as follows.

$$\begin{aligned} x_{\text{cp}} &= x_{\text{ref}} - \frac{C_{Mp}}{\text{target}C_L} \times \text{MAC} \\ x_{\text{ref}} &= 25\%\text{MAC} \end{aligned} \tag{1}$$

On the other hand, the center of gravity x_{cg} is computed from the aerodynamic center N_0 as follows.

$$\begin{aligned} x_{\text{cg}} &= N_0 - \text{const.} \\ &= x_{\text{ref}} - \frac{\Delta C_{Mp}}{\Delta C_L} \times \text{MAC} - \text{const.} \end{aligned} \tag{2}$$

C_{Mp} is pitching moment coefficient. where, the constant value const. in eq.(2) is defined by the results of Navier-Stokes computations in advance. It is set on 0.817[m] in this study.

2) Geometry Definition: The planform of the main wing and the configurations of the fuselage, the engine, the vertical tail wing, and stabilizer are fixed. The design variables for aerodynamic geometry are related to the airfoil shapes, the twist, the position relative to the fixed fuselage for the main wing as well as the deflection angle of the stabilizer. Airfoil shapes are defined at the root, kink, and tip of the main wing by using distribution of the thickness and the camber line. The twist center is defined at 80% chordwise position so that the straight hinge line for aileron is secured. The position of the wing root relative to the fuselage is parameterized by z coordinate (heightwise direction) of the leading edge, angle of attack, and dihedral. The entire computational aerodynamic geometry was thus defined by 50 design variables. The detail of the design variables is summarized in Table I.

TABLE I
DETAIL OF DESIGN VARIABLES. THE SERIAL NUMBER OF 1 TO 49 IS SET FOR THE MAIN WING, AND THE SERIAL NUMBER OF 50 IS SET FOR THE STABILIZER.

serial number	correspondent design variable	
1	z coordinate	at root leading edge
2	cant angle for attachment to fuselage	
3	dihedral angle	
4 - 15	control points for camber	root, kink, tip
16 - 45	control points for thickness	root, kink, tip
46 - 49	control points for twisting angle	47 is set at kink
50	reflection angle of stabilizer	

On the other hand, a structural geometry does not have one-to-one correspondence for an aerodynamic geometry. A structural geometry is uniquely determined by the objective function as the minimization of the main-wing weight W for an aerodynamic geometry. In the present study, the main wing separates the inboard and outboard wings using the threshold of the maximum wing thickness as 50.0[mm]. The inboard wing is compounded as multi-frame structure made from aluminum material. It is described by two design variables such as the thicknesses of skin and multi frames. The outboard wing is composed as full-depth honeycomb sandwich structure made from a composite material defined as symmetrical stacking $[0/\theta/{-\theta}/90]_{ns}$. θ is set as 15, 30, 45, 60, and 75deg. Whenever only one fiber angle is fulfilled for the structural requirements, the individual is judged to be satisfied with them. Hence, the total number of four design variables is used to describe the wing structural geometry. Note that these four design variables are subsidiary to 50 design variables for the aerodynamic geometry.

3) Constraints: The several geometrical constraints are considered as follows. The planform of the main wing is fixed. The maximum thickness of the main wing at root and kink has limit from 4% to 6% chord length. The maximum thickness at tip has also limit from 2% to 4% chord length. The camber line of main wing does not wave at root, kink, and tip. That is, a wavy surface wing is not considered. The twisting angle of the main wing is monotonously reduced at spanwise. The control point for twisting angle sets at kink. The generated main wing stays in the fuselage. The number of the symmetrical stacking n is set on $^{\forall}n \in \boldsymbol{N}^{+} \leq 25$. When n is greater than 25, the individual is not judged to be able to fulfill the structural requirements. Therefore, the penalty is imposed on the ranking in the optimizer.

B. Evaluation Method

The present optimization system provides three evaluation modules for aerodynamics, structures (including aeroelasticity), and boom noise. As the structures module uses the result of aerodynamic evaluation, these phases are carried out one by one. The master processing element (PE) manages the hybrid optimizer, while the slave PEs computed those three evaluation processes. Slave processes do not have to synchronize. It takes roughly seven days at least to evaluate one generation using 400CPUs of the Central Numerical Simulation System (CeNSS) of Numerical Simulator III in JAXA.

1) Aerodynamic Evaluation: In the present study, TAS-Code, parallelized unstructured Euler/Navier-Stokes solver using domain decompositions and message-passing interface library, is employed. The three-dimensional Euler equations are solved with a finite-volume cell-vertex scheme on the unstructured mesh[15] under supersonic flight condition. Taking advantage of the parallel search in the hybrid optimizer, the present optimization is parallelized. Moreover, the aerodynamic computation is also parallelized on the scalar machine.

2) Structural Evaluation: In the present MDO system, structural and aeroelastic optimization of the thickness of each multi-frame for inboard wing and the stacking sequence optimization of laminated composites for outboard wing are simultaneously performed to realize minimum W fulfilling the constraints of strength and flutter requirements. Given the wing outer mold line for each individual, finite element model is automatically generated from aerodynamic evaluation result of supersonic cruising condition, such as coordinates, pressure coefficient, and normal vectors (x, y, z, C_p, $x_{\perp}$, $y_{\perp}$, and $z_{\perp}$). The strength and flutter characteristics are evaluated by using the commercial software MSC. NASTRAN$^{\mathrm{TM}}$.

3) Sonic Boom Evaluation: The Computer-aided design-based Automatic Panel Analysis System (CAPAS)[16] is used to evaluate I_{boom}. CAPAS is a conceptual aerodynamic design tool in JAXA. This tool comprised four design processes as follows; 1) geometry definition of airplane component, 2) combination of all components in an airplane configuration using an application program interface for the CATIA$^{\mathrm{TM}}$V4, 3) generation of panel and aerodynamic analysis using panel method, 4) sonic-boom analysis using a modified linear theory.

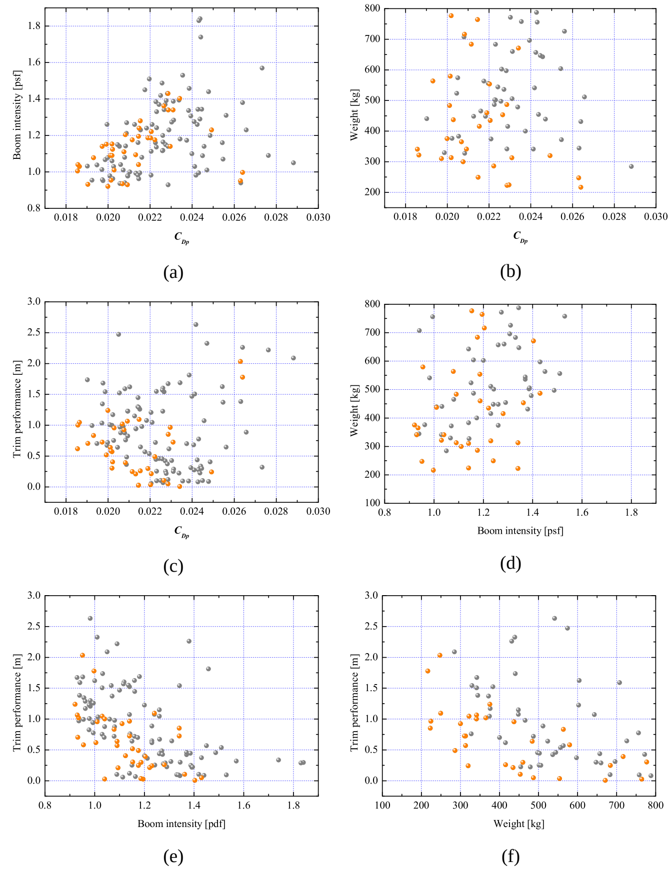

Fig. 3. All and derived non-dominated solutions on two dimensional planes between the objective functions. The non-dominated solutions are plotted by using orange color. Since these graphs are addressed to the practical design space, the number of orange-plot is not necessarily equal to that of non-dominated solution. (a)C_{D_p} vs. I_{boom}. (b) C_{D_p} vs. Weight. (c) C_{D_p} vs. Trim performance. (d) I_{boom} vs. Weight. (e) I_{boom} vs. Trim performance. (f) Weight vs. Trim performance.

As an aerodynamic evaluation module in CAPAS is low-fidelity because a geometry is inaccurate due to rough computational panel, the aerodynamic performance in CAPAS is used only to evaluate I_{boom}.

C. MDO Result

The population size was set on eight. It took roughly 20 hours of CPU time of CeNSS 50 processing elements (PEs) for an Euler computation. Also, it took roughly five minutes of CPU time of one PE for a NASTRAN flutter computation. The total evolutionary computation of 18 generations was performed using 139 individuals, and 37 non-dominated solutions were obtained. The evolution might not converge yet. However, evolution was stopped because several non-dominated solutions was sufficient as the candidate of a compromise solution.

Figure 3 shows the all and derived non-dominated solutions projected on two-dimensional plane between two objectives. These plots indicates the following tradeoff information. There is no tradeoff between C_{Dp} and I_{boom} because the fuselage geometry, which obtains low boom and low drag performance, was fixed in this MDO. C_{Dp}, I_{boom}, and W give similar effect on trim performance. When C_{Dp} is greater than roughly 0.0213, individual can trim independent on C_{Dp}. On the other hand, when C_{Dp} is lower than 0.0213, there is a tradeoff between C_{Dp} and trim performance. When I_{boom} is greater than approximately 1.04, individual can similarly trim independent on I_{boom}. On the other hand, when I_{boom} is lower than 1.04, there is a tradeoff between I_{boom} and trim performance. Also, when W is greater than roughly 500, individual can trim independent on W. On the other hand, when W is lower than 500, there is a tradeoff between W and trim performance. This fact indicates that there is no feasible tradeoff region in the present design space, because trim performance might have tradeoffs for the other objective functions. The information which there is tradeoff between I_{boom} and trim performance is important for the design process, because the purpose of the $\mathrm{S^3TD}$ is the demonstration of low-boom supersonic transport, and I_{boom} and trim performance should be better simultaneously for the practical design.

D. Data-Mining Result

The data mining was performed for 37 non-dominated solutions to obtain the information to select the compromise solution. The acquired design information was presented to the designers of roughly 20 persons. It was employed as the resource of decision making to determine a compromise solution which was the prototype of the $\mathrm{S^3TD}$ 3rd configuration.

The fruitful knowledge was that there is tradeoff between trim performance and all of the other three objective functions. The prime objective of the $\mathrm{S^3TD}$ is low-boom design and its experimental demonstration. For this reason, the designers decided that the improvement of sonic-boom intensity should have the priority (there is scope for improvement regarding trim performance by the redesign of stabilizer *etc.*). Therefore, the key information was how to restrain boom intensity.

The mining results regarding the restraint of boom intensity reveal that the cant angle for attachment to fuselage, the twist, and the bluntness of leading edge of main wing give effects on front boom. The reflection angle of stabilizer also gives on rear boom. The intensity of front boom is generally determined by nose geometry. When the design variables addressed by mining are unfavorable, the boom intensity from main wing is higher than that from nose. In addition, N-shape signature of sonic boom might generate due to the merger of the shock waves from nose and from main wing. Moreover, the expansion wave generated from the trailing edge of inner main wing should not erase the peak of positive pressure by the lifting surface of rear fuselage. That is, a selected compromise solution should have camber near the trailing edge of main wing to restrain rear boom. The knowledge acquired by using ANOVA and SOM is minutely described hereinafter.

1) Knowledge Acquired by Using ANOVA: The variance of the design variables and their interactions by ANOVA are shown in Fig. 4. Their proportions are shown, which are larger than 1% to the total variance. In the present ANOVA analysis, as the input data is discontinuous, scant data is redeemed by using a Kriging-based response surface. The information how the important design variable gives effect is insufficient on ANOVA. The aim of the ANOVA is to find out and address the important design variables.

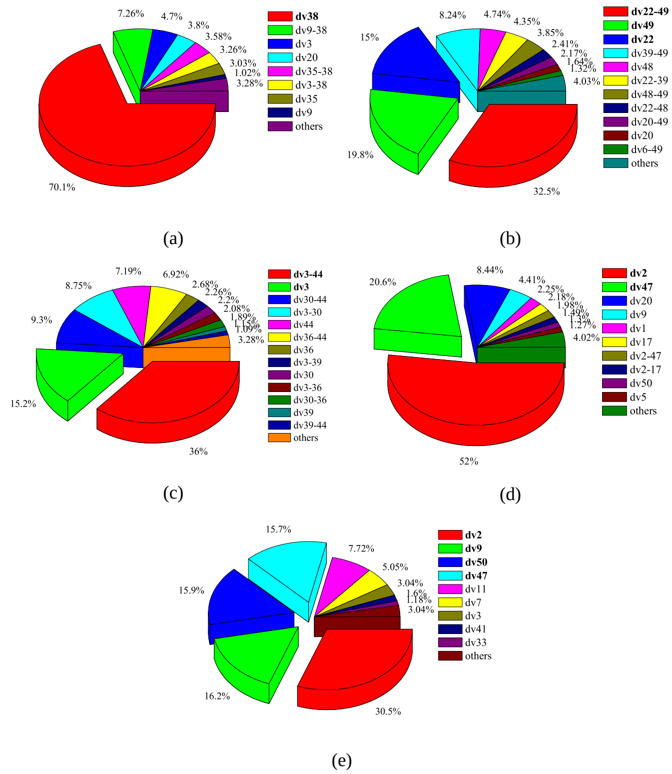

Fig. 4. Proportion of design-variable influence for the objective functions using ANOVA. 'dv' denotes the abbreviation of design variable. '-' indicates interaction between two design variables. Described numbers correspond to the serial number shown in Table I. (a) Result for C_{Dp}. (b) Result for boom intensity. (c) Result for structural weight using database including individuals not to fulfill the structural requirements. (d) Result for structural weight using database eliminating individuals not to fulfill the structural requirements. (e) Result for trim performance.

Figure 4 (a) shows the effect proportion of the design variables for C_{Dp}. This figure reveals that dv38 as the thickness in the vicinity of the leading edge at tip gives effect on C_{Dp}. Generally, when it becomes thick, C_{Dp} increases. When it becomes thin, C_{Dp} is decreased. Although the other wing thickness and leading-edge shape give effects on C_{Dp}, they does not have much effects because the perturbation is small in the 37 non-dominated solutions. That is, only dv38 can redesign for the reduction of C_{Dp} to keep an individual as a non-dominated solution.

Figure 4 (b) shows the effect proportion of the design variables for boom intensity. This figure reveals that dv22 and dv49 are important. dv22 represents the curvature of the wing surface at the rear location of maximum thickness. When this curvature is low, the rear boom achieves low. dv49 describes the twist angle at tip location. When this twist angle is large, as local angle of attack is negative, the front boom becomes large.

Two ANOVA works are performed for structural weight. One work employs the database including six individuals not to fulfill the structural requirements. Another work uses the database eliminating the six individuals not to fulfill the structural requirements. The result of the first case is shown in Fig. 4 (c). This result shows the information of design variables to fulfill the structural requirements. dv3 represents the angle of dihedral. This angle gives effect on the load distribution of the wing surface. dv44 describes the maximum thickness position at tip. When this value is small, as the thickness near the trailing edge is thin, the strength cannot be maintained. The result of the latter case is shown in Fig. 4 (d). This result shows the information of the design variables to reduce structural weight (; besides structural requirements are fulfilled). dv2 represents the angle of incidence of the wing. When this angle becomes large, the load distribution of the wing surface increases. dv47 describes the twist angle at kink. This angle also gives similar effect on the load distribution of the wing surface. As a constraint for the thickness to become non-dominated solution, the knowledge regarding the thickness of main wing is not obtained.

Figure 4 (e) shows the effect proportion of the design variables for trim performance. dv2 represents the angle of incidence of wing. As this angle gives effect on C_{Mp}, it is effective for trim performance. dv9 describes the curvature of the camber line near the leading edge at kink. When this design variable is large, as C_{Mp} increases, the body becomes instable. dv50 represents the reflection angle of the stabilizer. This angle gives similar effect to dv2 and dv9. dv47 describes the twist angle at kink. This angle also gives similar effect to dv2, dv9, and dv50.

2) Knowledge Acquired by Using SOM: The SOM is generated by using 37 non-dominated solutions to obtain the design knowledge to improve a compromise solution while it keeps the performance as a non-dominated solution. Figure 5 shows the generated SOM and colored maps by the four objective functions. The color pattern of them shows the tradeoffs among the four objects. The tradeoff information is summarized in Table II. This result reveals that trim performance is the important objective to determine the performances of the other objectives. That is, the present design space does not have the feasible tradeoff region. When trim performance is improved, all of the other objectives becomes absolutely worse.

Figure 6 shows the color maps by the important design variables addressed by ANOVA. The effective design variables for C_{D_p} are dv38 and dv9. Figures 5 (b) and 6 (e) reveal that large dv38 value increases C_{D_p}. Small dv38, however, does not improve C_{D_p} necessarily. Although there is no correlation between dv9 and C_{D_p} shown by the comparison between Figs. 5 (b) and 6 (c), dv9 should be small to become a non-dominated solution.

The effective design variables for I_{boom} are dv22 and dv49. The comparison between Figs. 5 (c) and 6 (d) reveals that small dv22 reduces boom intensity, though large dv22 does not increase I_{boom}. Although there is no correlation between dv49 and I_{boom} shown by the comparison between Figs. 5 (c) and 6 (h), dv49 should be small to become a non-dominated solution.

TABLE II
SUMMARIZATION OF THE TRADEOFF INFORMATION AMONG THE FOUR OBJECTIVE FUNCTIONS OBTAINED BY THE COLOR PATTERN ON SOM. ○ DENOTES THAT THERE IS TRADEOFF. ON THE OTHER HAND, × MEANS THAT THERE IS NO TRADEOFF.

	C_{D_p}	I_{boom}	W	$\lvert x_{\text{cp}} - x_{\text{cg}}\rvert$
C_{D_p}	╲	×	○	○
I_{boom}	—	╲	×	○
W	—	—	╲	○
$\lvert x_{\text{cp}} - x_{\text{cg}}\rvert$	—	—	—	╲

The effective design variables for W are dv3 and dv44 when the all 37 solutions included the individuals not to fulfill the structural requirements consider. That is, the good design of dv3 and dv44 generates the solution to fulfill the structural requirements. The comparison between Figs. 5 (d) and 6 (b) reveals that large dv3 improves the weight of the main wing, although small dv3 increases the W. On the other hand, the comparison between Figs. 5 (d) and 6 (f) shows that small dv44 improves weight, although large dv44 has no correction. The effective design variables for W are dv2 and dv47 when the solutions eliminated the individuals not to fulfill the structural requirements consider. The comparison between Figs. 5 (d) and 6 (a) reveals that small dv2 improves W, although large dv2 increases W. On the other hand, the comparison between Figs. 5 (d) and 6 (g) shows that small dv47 improves weight, although large dv44 increases W.

The effective design variables for trim performance are dv2, dv9, dv50, and dv47. The comparison between Figs. 5 (e) and 6 (a) reveals that large dv2 improves trim performance, although small dv2 becomes trim performance worse. The comparison between Figs. 5 (e) and 6 (c) reveals that small dv2 is the necessary condition to improve trim performance. The comparison between Figs. 5 (e) and 6 (i) reveals that large dv50 becomes trim performance worse. The comparison between Figs. 5 (e) and 6 (g) reveals that large dv47 improves trim performance, although small dv47 becomes trim performance worse.

Since there are tradeoffs between trim performance and all of the other objective functions, the design variables as dv2, dv9, and dv50 effecting trim performance determine the tradeoff among the objective functions.

E. Selection and Evaluation of Compromise Solution

The individual shown in Fig. 7 is selected using the information obtained by design-informatics approach. The concrete presented materials roughly classify into two groups. One is the information regarding the tradeoffs among the objective functions shown in Fig. 3. The SOMs shown in Fig. 5 are also produced because they corroborate the tradeoffs. The other is the information concerning the candidates of a compromise solution. This includes the contour figure of C_p distribution at the supersonic cruising condition, the specifications (as the

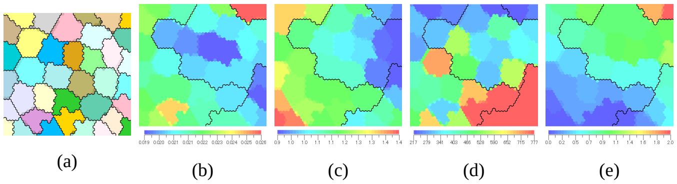

Fig. 5. The resulting SOM separated by 37-non-dominated-solution region and SOMs colored by the objective functions. (a) SOM separated by 37-non-dominated-solution region. (b) colored by C_{D_p}. (c) by I_{boom}. (d) by W. (e) by $|x_{\text{cp}} - x_{\text{cg}}|$

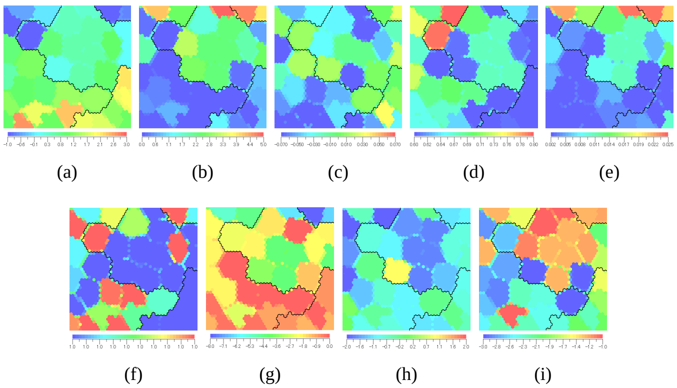

Fig. 6. SOMs colored by the design variables which are indicated by ANOVA. (a) colord by dv2. (b) by dv3. (c) by dv9. (d) by dv22. (e) by dv38. (f) by dv44. (g) by dv47. (h) by dv49. (i) by dv50.

objective-function values, number of laminations for composite material, thickness of aluminum material, the design angle of attack, and the reflection angle of the stabilizer), the wing section and C_p distribution at root, kink, and tip, the spanwise C_L, C_D, and twisting angle, the ground pressure signature, and the velocity-damping and velocity-frequency curves at each computational condition to seek the flutter speed. Besides, the candidates are selected from the non-dominated solutions and individuals adjacent to them on Fig. 3 (e), which indicates the relation between the boom intensity and the trim performance. The boom intensity has priority in this study. The trim performance gives tradeoffs for all of the other objective functions. The individual with disadvantageous manufacturing problem is excepted from the candidates. The important points are 1) the performance of all objective functions and 2) the possibility for the improvement of the other three objectives to keep the boom performance. On the final decision of a compromise solution, the individual which the wing section to be alike NEXST-1 was selected. That is, the shape of the selected compromise solution convinces regarding aerodynamics and manufacture. The trim performance was concluded to be improved by the regulation of the reflection angle of stabilizer (the outside range set in the present optimization is namely reconsidered). Therefore, a weak non-dominated solution was ventured to select for a compromise solution.

Table III shows the specification of the compromise solution. It is notable that the criteria of the design angle of attack and the reflection angle of stabilizer is the horizontal line (longitudinal axis of body) for three views. Thus, the

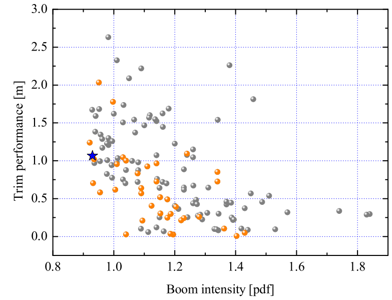

Fig. 7. Location of compromise solution projected onto two dimensional plots between boom intensity and trim performance. The star plot denotes the selected compromise solution.

TABLE III

THE SPECIFICATION OF THE SELECTED COMPROMISE SOLUTION.

C_{D_p}	0.02092
I_{boom}	0.9301 [psf]
W	341.3 [kg]
$\lvert x_{\text{cp}} - x_{\text{cg}}\rvert$	1.065 [m]
outboard wing	8plies $\times$ 4 sets
inboard wing	skin: 9.0 [mm], multi frames: 8.9 [mm]
design angle of attack	2.915 [deg]
reflection angle of stabilizer	-1.608 [deg]

reflection angle is defined for longitudinal axis of body and is independent of angle of attack. This result shows that the trim performance is insufficient. The results from ANOVA shown in Fig. 4 indicate that the cant angle (dv2) and the geometry (dv9 and dv47) of the main wing which are influent in the trim performance give effects on several objective function. However, the reflection angle of the stabilizer does not give effect on any objective functions except the trim performance. Since the designed reflection angle of the stabilizer can afford to be harder, the modification of it can improve the trim performance.

Figure 8 shows the C_p distributions on upper surface and on symmetrical plane. This figure reveals that the shock waves occur around the front location of the engine and bumps into the upper surface of the main wing. Although the shock wave is shielded, the performance of the wing is down. It is important to design the geometry of the wing for the alleviation of this shock wave.

Figure 9 shows the C_p distributions and the wing sections at root, kink, and tip location. At the root location, since two shock waves bump into the wing upper surface, the increase of the wing thickness obtains insufficient lift performance and augment the induced drag. On the other hand, it reveals the connection between the structural weight and the structural requirements. The constraint of the thickness at root is 5%±1% chord length. The thickness of the compromise solution at root is 4.4% chord length. The thickness of the compromise solution becomes thin with the fulfillment of the structure requirements. At the kink location, upper surface near leading edge dents, because this depression moderates the shock wave occurred from the front of the engine. This hollow is the

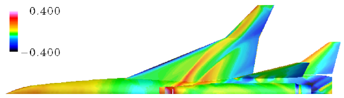

(a) Upper surface view

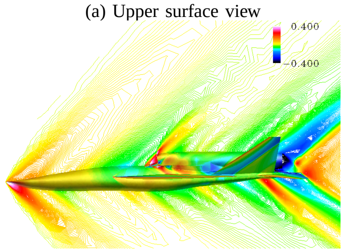

(b) Symmetrical-plane view

Fig. 8. C_p distribution of the decided compromise solution. The angle of attack of 2.915deg is set to achieve the target C_L.

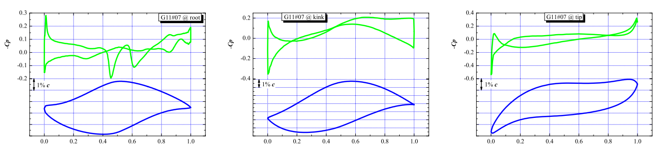

(a) Airfoil shape at root (21.62% spanwise location) (b) Airfoil shape at kink (63.33% spanwise location) (c) Airfoil shape at tip (99.00% spanwise location)

Fig. 9. C_p distribution and airfoil shape of the decided compromised solution at root, kink, and tip locations of main wing. c is chord length.

key to improve the aerodynamic performance. The maximum thickness at kink is 5.4% chord length. The thickness at kink location should be simultaneously thick to have sufficient aerodynamic performance and to fulfill the structural requirements. At the tip location, the wing has insufficient aerodynamic performance. Since the wing geometry in the vicinity of the tip gives strict effects on the boom intensity indicated by the data-mining results, the wing tip geometry is evolved to reduce the boom intensity. In addition, the strong shock wave occurs around the rear part of the fuselage. As this corrupts the rear boom intensity, the re-consideration is needed.

IV. Conclusion

The design-informatics approach has been proposed for the efficient design, in which the construction of the design database is implemented and the design information is extracted from it. This information systematizes the design space, and assists the efficient selection of a compromise solution. In the present study, the approach has been applied to the intimate configuration of the silent supersonic technology demonstrator projected by Japan Aerospace Exploration Agency for the conceptual design of the 3rd configuration of the silent supersonic technology demonstrator under the design requirements among the aerodynamic, stability, sonic-boom, structural, and trim performances. The process of the approach gave the tradeoffs among the defined design requirements, *i.e.*, objective functions. Thereby, it was revealed that the improvement of trim performance corrupts the other requirements. Furthermore, the important design variables were evident, and the correlations between the design requirements and them were also shown. The obtained design information was produced to the designers and it was employed as the resource of decision making to determine a compromise solution. The knowledge was produced for the future design. The design-informatics approach is an efficient and effective design manner, and moreover it can pursue an innovative and creative design.

Acknowledgments

The authors would first like to thank all members of the supersonic transport team in aviation program group, JAXA for providing useful advice. The Euler/NASTRAN computations were performed by using the CeNSS of Numerical Simulator III in JAXA's engineering digital innovation(JEDI) center, JAXA. We would also like to thank Ms. Masako Tsuchiya and Mr. Masahiro Yoshida, the managers in JEDI center, for their kind help regarding the CeNSS employment. This research was partially supported by the Ministry of Education, Science, Sports and Culture, Grant-in-Aid for Young Scientists (B) 22700155, 2010.

References

[1] A. Samad, K. Kim, T. Goel, R. T. Haftka, and W. Shyy, "Multiple surrogate modeling for axial compressor blade shape optimization," *Journal of Propulsion and Power*, vol. 24, no. 2, pp. 302–310, 2008.
[2] A. Murakami, "Silent supersonic technology demonstration program," 2006, *Proceedings on 25th International Council of the Aeronautical Sciences*, ICAS 2006-1.4.2, Hamburg, Germany, 2006.
[3] K. Chiba and S. Obayashi, "Knowledge discovery in aerodynamic design space for flyback-booster wing using data mining," *Journal of Spacecraft and Rockets*, vol. 45, no. 5, pp. 975–987, 2008.
[4] K. Chiba, Y. Makino, and T. Takatoya, "Pso/ga hybrid method and its application to supersonic-transport wing design," *Journal of Computational Science and Technology*, vol. 2, no. 1, pp. 268–280, 2008.
[5] S. Jeong, S. Hasegawa, K. Shimoyama, and S. Obayashi, "Development and investigation of efficient ga/pso-hybrid algorithm applicable to real-world design optimization," in *IEEE Computational Intelligence Magazine*, August 2009, pp. 36–44.
[6] A. J. Keane, "Wing optimization using design of experiment, response surface, and data fusion methods," *Journal of Aircraft*, vol. 40, no. 4, pp. 741–750, 2003.
[7] S. Jeong, M. Murayama, and K. Yamamoto, "Efficient optimization design method using kriging model," *Journal of Aircraft*, vol. 42, no. 2, pp. 413–420, 2005.
[8] S. Obayashi and D. Sasaki, "Visualization and data mining of pareto solutions using self-organizing map," in *The 2nd International Conference on Evolutionary Multi-Criterion Optimization, LNCS 2632*, Springer-Verlag Heidelberg, Faro, Portugal, 2003, pp. 796–809.
[9] C. M. E. Holden and A. J. Keane, "Visualization methodologies in aircraft design," 2004, aIAA Paper 2004-4449, 2004.
[10] I. M. Sobol, "Sensitivity estimates for nonlinear mathematical models," *Mathematical Modelling and Computational Experiments*, vol. 1, no. 4, pp. 407–414, 1993.
[11] D. R. Jones, M. Schonlau, and W. J. Welch, "Efficient global optimization of expensive black-box functions," *Journal of Global Optimization*, vol. 13, no. 4, pp. 455–492, 1998.
[12] T. Kohonen, *Self-Organizing Maps*. Springer, Berlin, Heidelberg, 1995.
[13] T. Ohnuki, K. Hirako, and K. Sakata, "National experimental supersonic transport project," 2006, *Proceedings on 25th International Council of the Aeronautical Sciences*, ICAS 2006-1.4.1, Hamburg, Germany, 2006.
[14] K. Chiba, Y. Makino, and T. Takatoya, "Evolutionary-based multidisciplinary design exploration for silent supersonic technology demonstrator wing," *Journal of Aircraft*, vol. 45, no. 5, pp. 1481–1494, 2008.
[15] Y. Ito and K. Nakahashi, "Direct surface triangulation using stereolithography data," *AIAA Journal*, vol. 40, no. 3, pp. 490–496, 2002.
[16] Y. Makino and Y. Naka, "Sonic-boom research and low-boom demonstrator project in jaxa," 2007, *Proceedings on 19th International Congress on Acoustics*, NLA-08-002-IP, Madrid, Spain, 2007.